3.5.11

MAGIC chopper: basic concept and experimental evaluation

M. Nakamura[1], K. Ikeuchi[2], R. Kajimoto[1], W. Kambara[1], Th. Krist[3], T. Shinohara[1], M. Arai[1], K. Iida[2], K. Kamazawa[2], Y. Inamura[1] and M. Ishikado[2]

[1] Materials and Life Science Division, J-PARC Center, Japan Atomic Energy Agency, Tokai, Ibaraki 319-1195, Japan
[2] Research Center for Neutron Science and Technology, Comprehensive Research Organization for Science and Society, Tokai, Ibaraki 319-1106, Japan
[3] Helmholtz Zentrum Berlin for Materials and Energy, Hahn-Meitner-Platz 1, 14109 Berlin, Germany

E-mail: mitsutaka.nakamura@j-parc.jp

Abstract. The efficiency of inelastic neutron scattering measurement by a chopper spectrometer can be markedly improved by utilizing multiple incident energies (Multi-E_i method). However, in conventional chopper system, the optimization of experimental condition for all the incident energies is absolutely impossible. We have proposed and developed a new Fermi chopper with supermirror-coated slitpackage, so-called MAGIC chopper, in order to overcome the problem. The nearly full optimization of experimental condition for Multi-E_i method using a prototype of MAGIC chopper has been experimentally demonstrated.

1. Introduction

Inelastic neutron scattering (INS) measurements by chopper spectrometers at pulsed spallation neutron sources have greatly contributed to the development of materials science. There, a sample is irradiated by incident neutron beam monochromated by a mechanical chopper, and the momentum transfer (Q) and energy transfer (E) in the sample are detected by time-of-flight (TOF) technique. A high incident energy (E_i) measurement provides us the dynamical properties in a wide Q-E range, while a low E_i measurement more precise information on dynamical properties although the coverage of Q-E range becomes narrow. Chopper spectrometers should remain to be flagship instruments in the new generation pulsed neutron sources such as Japan Proton Accelerator Research Complex (J-PARC). However, an INS measurement has a drawback in measurement efficiency. Due to the faint signal of inelastic process, long measurement time and a large amount of sample have been needed to acquire a good-quality INS data. This situation prevented us from carrying out INS measurements under various experimental conditions within a limited beam time, and has been an impediment to progress in materials science.

Conventional INS measurements by a chopper spectrometer at a pulsed neutron source utilize single monochromatic incident beam. On the other hand, several E_i beams are delivered to the sample within 1-frame of a period of the pulsed source, because the rotating frequency of monochromating chopper is usually much higher than the frequency of the pulsed source. In other words, a single E_i experiment has wasted the other incident neutrons and yielded a long

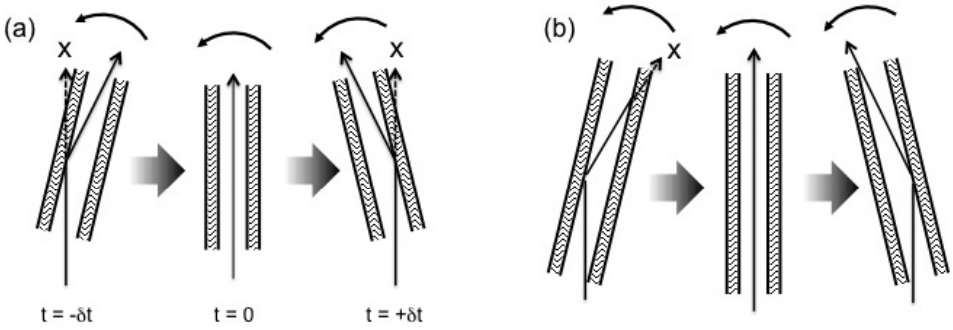

Figure 1. Schematic illustration of (a) MAGIC chopper concept and (b) the relation between the rotating slits and the reflected neutrons.

dead-time on a TOF measurement. If we can utilize the multiple E_i's inherently selected by the chopper, the efficiency of an INS measurement should be significantly improved [1, 2, 3, 4]. Previously, we succeeded in demonstrating that multiple two-dimensional maps of a dynamical structure factor in Q-E space are simultaneously obtained by one measurement using the Fermi chopper spectrometer 4SEASONS [5] which is installed at BL01 of the Materials and Life Science Experimental Facility (MLF) in J-PARC. We refer to this technique used in J-PARC as Multi-E_i method. This technique has been already in widespread use at J-PARC [6, 7, 8]. However, it must be noted that the Multi-E_i method in a conventional chopper spectrometer involves a crucial problem. Usually, the chopper opening time Δt_ch is tuned to the pulse width emitted from moderator Δt_m, because the relation of $\Delta t_\mathrm{m} \approx \Delta t_\mathrm{ch}$ is an optimized condition for INS measurement by a chopper spectrometer. The Δt_m depends on neutron energy and the Δt_ch of a conventional chopper keeps constant at all times, and so the Multi-E_i method using a conventional chopper cannot realize the optimized experimental condition for each of incident energies. The lower incident energy measurement in Multi-E_i method realizes better energy resolution at the expense of intensity. The pulse peak intensity of neutron source in J-PARC reach a maximum at a relatively low-energy region ($\sim$ 10 meV), and thus the lower energy measurement in Multi-E_i method should be highly significant even if the intensity is sacrificed. However, the higher incident energy measurement in Multi-E_i method often causes a worthless result due to the worse energy resolution.

In order to overcome the optimization problem in Multi-E_i method, we proposed a new Fermi chopper with supermirror-coated straight slits (MAGIC chopper). We have developed a prototype of MAGIC chopper, and carried out the transmittance experiment on pulsed neutron beam at J-PARC. This paper describes the basic concept [9] and the experimentally-confirmed performance [10] of a rotating supermirror-coated slit package. The feasibility of high efficient INS measurement with MAGIC chopper is also discussed.

2. Basic concept of MAGIC chopper

2.1. Energy dependent chopper opening time

Supermirror has characteristic features associated with neutron wavelength. That is, larger critical angle is allowed for the incidence of neutron with longer wavelength. With the aid of supermirror on the surface of the transmitters we can make efficient use of neutrons with the MAGIC chopper which were doomed to be unavailable with a conventional chopper as shown in Fig. 1(a). The block arrows in Fig. 1 denote the evolution of time. The effective chopper

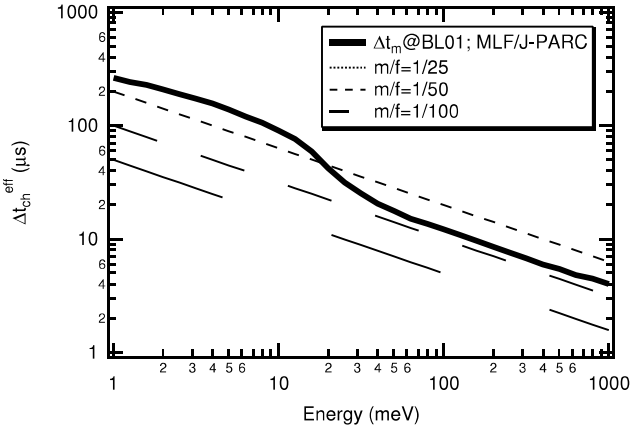

Figure 2. Energy dependent chopper opening time $\Delta t_{\rm ch}^{\rm eff}$ for several m/f cases.

opening time $2\delta t$ depicted in Fig. 1(a) can be written as

$$2\delta t = \Delta t_{\rm ch}^{\rm eff} = 2 \times \frac{1.73 m \lambda_{\rm i}}{2\pi f} \times 10^3 (\mu{\rm s}), \tag{1}$$

where m is the m-value of the supermirror, f (Hz) the chopper frequency, and the term $1.73 m\lambda_{\rm i}$ (mrad) corresponds to the critical angle for incident neutron $\lambda_{\rm i}$ (Å). This equation means that the chopper opening time can be effectively extended for longer neutron wavelength. From the expression of Eq. (1) the ratio m/f is an important parameter to adjust the behavior of $\Delta t_{\rm ch}^{\rm eff}$. It should be noted that the rotating slits with the finite depth block the reflected neutrons in case that the reflection direction is opposite to the rotation direction. The relation between the rotating slits and the reflected neutrons are shown in Fig. 1(b). The practical case of this effect will be described in Sec. 4. Figure 2 shows the energy dependencies of $\Delta t_{\rm ch}^{\rm eff}$ for several m/f cases. The data of energy dependent $\Delta t_{\rm m}$ for 4SEASONS, which is downloaded from the web page [11], is also included in the figure for comparison. Let us stress that the *energy dependent* $\Delta t_{\rm ch}$ can be realized by MAGIC chopper.

For high energy neutrons, the angular divergence defined by the chopper geometry should determine the chopper opening time. Consider a rotating single slit of width w (mm), depth D (mm), and frequency f (Hz). The chopper opening time originated in the slit divergence is

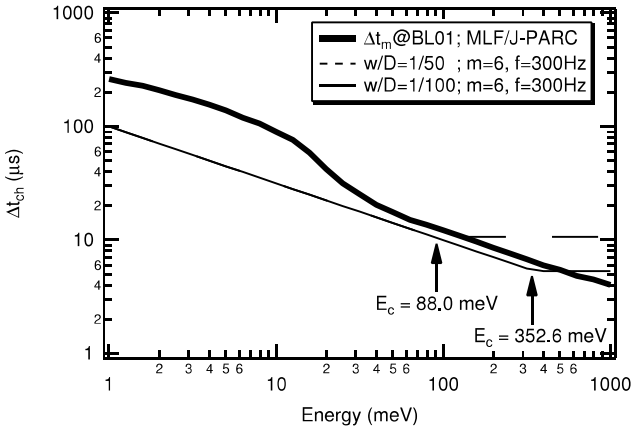

Figure 3. Energy dependent chopper opening time for two different w/D cases. In this figure we assume $m = 6$ and f=300 Hz.

given by

$$\Delta t_{\rm ch}^{\rm div} = \frac{w}{2\pi D f} \times 10^6 [\mu{\rm s}]. \tag{2}$$

Thus, we can estimate the crossover wavelength $\lambda_{\rm c}$ from the condition of $\Delta t_{\rm ch}^{\rm eff} = \Delta t_{\rm ch}^{\rm div}$,

$$\lambda_{\rm c} = \frac{1000}{3.46m} \cdot \frac{w}{D} [\text{Å}]. \tag{3}$$

As seen in Eq. (3) the ratio w/D is a parameter to define the crossover wavelength (energy). The energy dependent chopper opening times $\Delta t_{\rm ch}$ for two different chopper divergences (w/D = 1/50 and 1/100) are represented in Fig. 3. We assumed the condition of $m = 6$ and f = 300 Hz in this figure. Under the condition of $m = 6$, the ratio $w/D = 1/50$ (20 mrad) yields $\lambda_{\rm c}$ = 0.96 Å($E_{\rm c}$ = 88 meV), and $w/D = 1/100$ (10 mrad) gives $\lambda_{\rm c}$ = 0.48 Å($E_{\rm c}$ = 352.6 meV). It is obvious that the smaller angular collimation shifts the crossover energy towards higher energy region.

2.2. Nearly constant energy resolution

For a chopper spectrometer, the energy resolution at elastic position can be expressed as

$$\frac{\Delta E}{E_{\rm i}} = \left[\left\{ 2\frac{\Delta t_{\rm ch}}{t_{\rm c}} \left(1 + \frac{L_1}{L_2} \right) \right\}^2 + \left\{ 2\frac{\Delta t_m}{t_{\rm c}} \left(1 + \frac{L_3}{L_2} \right) \right\}^2 \right]^{1/2}, \tag{4}$$

where $E_{\rm i}$ is the incident energy of neutrons, $\Delta t_{\rm ch}$ the chopper opening time, $\Delta t_{\rm m}$ the pulse width at the moderator, $t_{\rm c}$ the traveling time of incident neutron from moderator to monochromating chopper, L_1 the distance from moderator to sample, L_2 the distance from sample to detector, and L_3 the distance from monochromating chopper to sample.

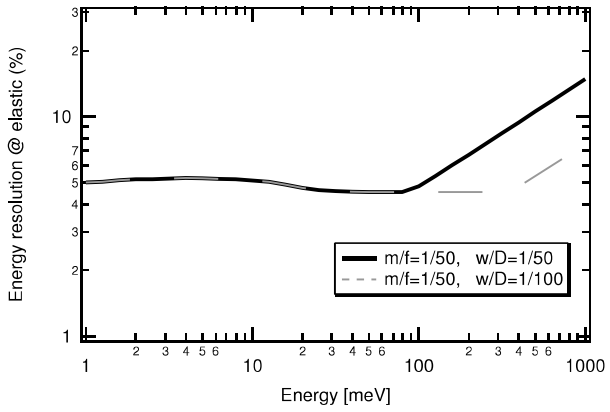

Figure 4. Calculated energy resolutions at elastic position for several chopper configurations.

According to the instrumental parameter of 4SEASONS, L_1 = 18 m, L_2 = 2.5 m, and L_3 = 1.8 m[14]. By substituting the energy dependent chopper opening time into $\Delta t_{\rm ch}$ in Eq. (4), we can estimate the energy resolution of 4SEASONS equipped with MAGIC chopper. Calculated energy resolutions for several cases are shown in Fig. 4. In case of the $m/f = 1/50$ and $w/D = 1/100$ configuration, the energy resolution becomes almost constant ($\sim 5\%$) in the wide range of incident energy 1 − 300 meV. This is a consequence of the energy dependence

of effective chopper opening time, that is $\Delta t_{\rm ch} \propto 1.73 m\lambda_{\rm i} \propto E_{\rm i}^{-1/2}$. Therefore, all the energy dependent terms in Eq. (4) are cancelled out since $t_{\rm c}$ is proportional to $E_{\rm i}^{-1/2}$ and $\Delta t_{\rm m}$ follows a $E_{\rm i}^{-1/2}$ variation in a wide energy range.

3. Experimental evaluation

3.1. Slit package

Two types of slit packages, one with and the other without neutron supermirrors, were prepared in order to investigate the characteristic properties of a supermirror-coated slit package. The slit package without neutron supermirrors was composed of alternating Si and ^{10}B layers. The Si wafers, of thickness 150 μm, transmit neutrons, whereas the ^{10}B, of thickness $\sim$15 μm, is a strong absorber. In the case of the slit package with neutron supermirrors, both sides of the Si wafers were coated with Ni/Ti supermirrors with $m = 3$. The slit packages were fixed by a holder as shown in Fig. 5. Unnecessary transmitting neutrons resulting from the shorter depth of a slit package (17 mm) than the width of the beam window (30 mm), can be shielded by the Cd plates, of thickness 0.5 mm, which are inserted at the both lateral sides of a slit package.

3.2. Rotation testing machine

We have developed a rotation testing machine in-house to investigate the performance of rotating slit packages. A holder containing a slit package was inserted in a rotor body made of aluminum. Balance adjustment of rotor-body and holder complex was made by a balancing machine. Figure 6 shows a photograph of the rotation testing machine. The rotation was driven by a servomotor with mechanical bearings, and it was synchronized with a trigger signal at the repetition rate of the pulsed neutron source. The rotor body and holder complex were rotated by the rotation testing machine, and the maximum rotation frequency was designed to be 150 Hz.

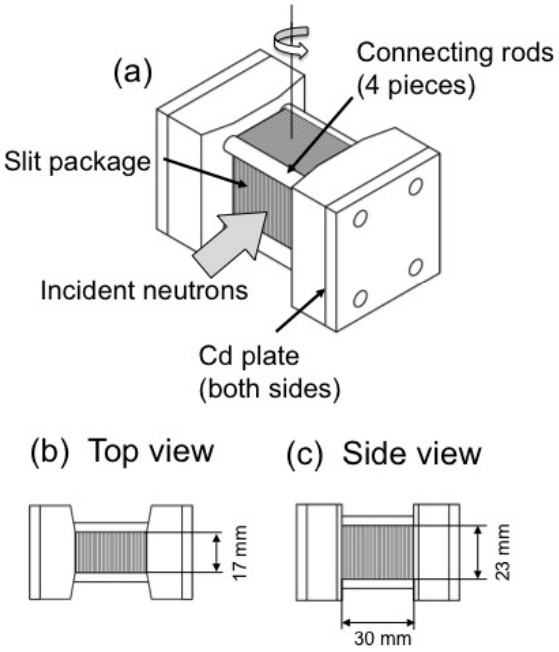

Figure 5. Schematic drawings of a slit package; (a) diagrammatic perspective view, (b) top view and (c) side view.

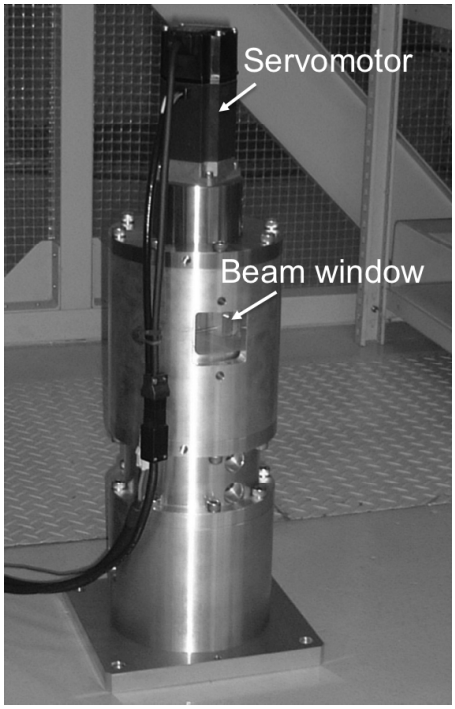

Figure 6. Photograph of a rotation testing machine.

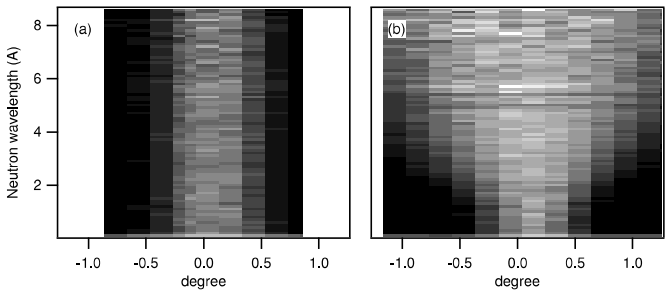

Figure 7. Two-dimensional maps of rocking curve measurement for slit packages (a) without and (b) with neutron supermirrors ($m = 3$).

3.3. Transmittance experiment

Neutron transmittance experiments were carried out on NOBORU (BL10 of MLF) which is designed to study neutronic performance of the spallation neutron source system of J-PARC and to provide a test beam port to promote research and development on innovative neutron devices [12, 13]. In this study, we performed two kinds of transmittance experiments to evaluate the performance of slit packages with and without neutron supermirrors.

One of the experiments performed was the rocking curve experiment. This experiment was performed to study the *static* properties of the slit packages. In the experiment, a pulsed white neutron beam was delivered to the slit package, which was placed on a goniometer located 13,400 mm from the neutron moderator. The band definition chopper was used for frame overlap suppression. The transmitted beam was detected at a ^{3}He neutron beam monitor made by LND, Inc. which was situated 13,700 mm from the neutron moderator. The size of the incident beam was 20 mm $\times$ 20 mm at the center of the slit package.

The other experiment was the synchronous rotation experiment. In this experiment, the rotation was synchronized with the repetition rate of the pulsed neutron source to elucidate the *dynamic* properties of the slit packages. The rotation testing machine incorporating the slit package was located 13,400 mm from the neutron moderator. The rotation frequency was 100 Hz for the two different slit packages, with and without neutron supermirrors; the phase delay was identical for each measurement. The size of the incident white beam size was 10 mm $\times$ 10 mm at the center of the slit package. The transmitted neutrons were detected by a two-dimensional neutron detector, which consisted of a position sensitive photomultiplier tube with a ZnS(Ag)/^{6}LiF scintillator on the surface. Information about the position and the arrival time of the neutron was recorded for each event. The detector surface was located 13,880 mm from the neutron moderator.

4. Results and discussions

Two dimensional maps of rocking curve measurements are given in Fig. 7. Collected TOF data are converted to the neutron wavelength dependent data by the following relation,

$$\lambda = 3.956 \times \frac{t}{L}(\text{Å}), \tag{5}$$

where t (μs) is the TOF at the detector, and L (mm) the distance from moderator to detector. The width of the time (wavelength) bin was 346 μs (0.1 Å). Figure 8 shows the one dimensional plots of rocking curve measurement for various incident wavelength regions, where the intensity was averaged over a certain range of incident wavelength. Transmitted neutron intensity in Fig. 8 are normalized by the direct beam intensity, obtained by removing the slit package from the path of neutron beam.

As expected, the peak width for the supermirror-coated slit package grew wider in direct proportion to the wavelength. This is due to the fact that a larger critical angle is allowed for

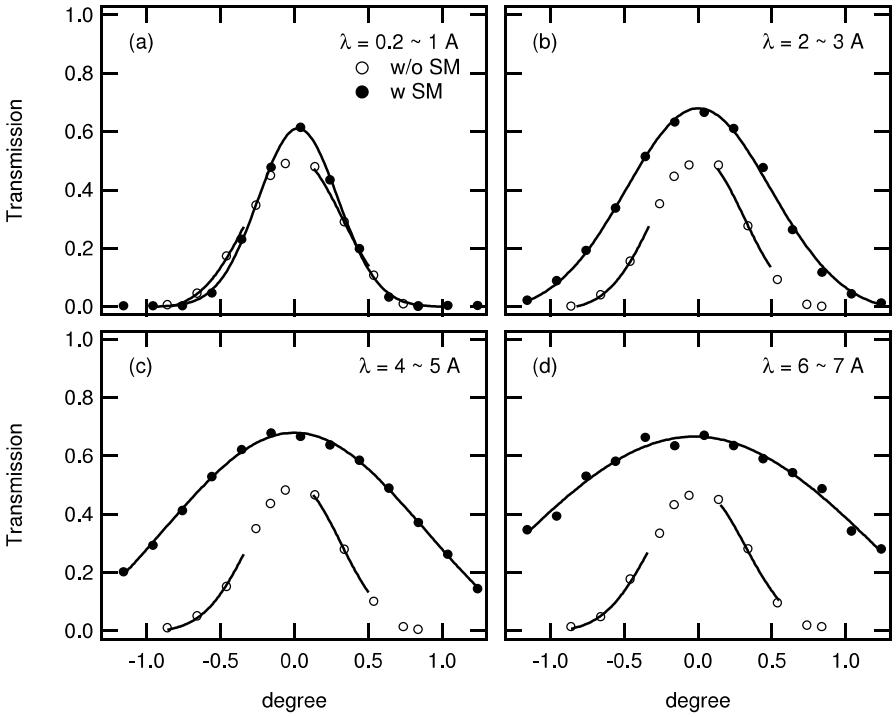

Figure 8. One dimensional plots of rocking curve measurement for slit packages with and without neutron supermirrors ($m = 3$). The intensity was averaged over a certain range of incident wavelength and normalized by the direct beam intensity measurement. Various ranges of incident wavelength are shown in the figures.

the longer wavelength neutrons. On the other hand, the peak height for the supermirror-coated slit package was found to be greater than that for the slit package without neutron supermirrors. This was an unexpected finding. The neutron supermirrors in the slit packages play an important role not only in the extension of effective chopper opening time, but also in the focusing of the divergent neutron beams.

Next, we discuss the synchronous rotation experiment. Figure 9 shows the TOF spectra of transmitted neutrons, both with and without supermirrors; the rotation frequency was 100 Hz, and the phase delay was identical for both slit packages. Intensities given in Fig. 9 are normalized by the direct beam intensity measurement. In the case of 100 Hz rotation without neutron supermirrors, we can observe several peaks at every ~ 5179 μs, which corresponds to one-half of the rotation period at the detector position, i.e., $1/100 \times 1/2 \times 13,880/13,400 \times 10^6 \mu$s. There was little difference between the two slit packages in the shorter TOF region (higher energy region). However, the differences were clear in the lower-energy region where for the slit package with the neutron supermirror, the intensity distribution widened and shifted toward the longer TOF side, unlike the case of the slit package without neutron supermirrors. The increase in the peak height for the supermirror-coated slit package was also confirmed in the synchronous rotation experiment. The intensity distribution in the supermirror-coated slit package can be explained by the relation between the rotation direction of slit package and the reflection direction of the neutrons shown in Fig.1(b). In the longer-TOF region depicted on the right-hand side of Fig. 1(b), the slits move in the same direction as the reflected neutron. In other words, the

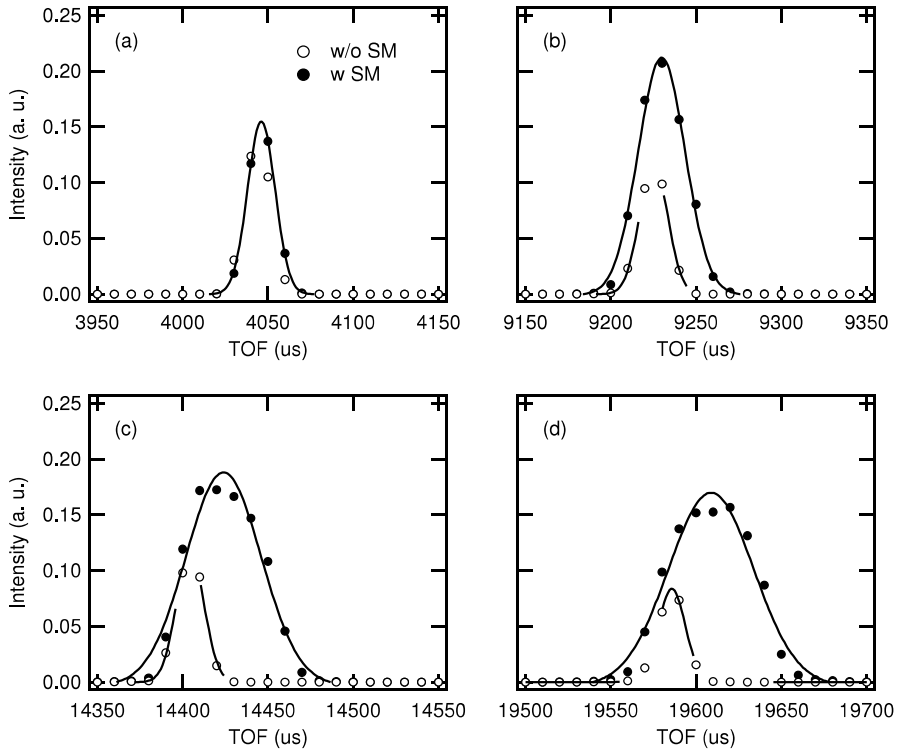

Figure 9. The TOF spectra of transmitted neutrons from rotating slit packages with and without neutron supermirrors ($m = 3$). The rotation frequency is 100 Hz for both the cases.

rotating slits provide a passage to the reflected neutrons. On the other hand, in the shorter-TOF region illustrated on the left-hand side of Fig. 1(b), the rotating slits block the reflected neutrons because the reflection direction is opposite to the rotation direction.

The width of the pulse transmitted by a rotating slit package, $\Delta t_{\rm ch}$, can be estimated from the observed pulse width at a detector, $\Delta t_{\rm d}$, as shown in Fig. 9,

$$\Delta t_{\rm ch} = \Delta t_{\rm d} \times (13,400/13,880), \tag{6}$$

where 13,400 mm is the distance from moderator to slit package, and 13,880 mm is the distance from moderator to the detector. Two pulse widths transmitted by the slit packages with and without neutron supermirrors are plotted in Fig. 10. The pulse width of supermirror-coated slit package decreases with neutron energy. This feature is exactly the essential characteristic of MAGIC chopper. The calculated result for $m = 3$ and $f = 100$ Hz in Eq. (1) is also plotted in Fig. 10. These experimental results are in good agreement with the calculated result.

Let us consider the energy resolution under the assumption that the supermirror-coated slit package used in this study is installed in the Fermi chopper spectrometer 4SEASONS at J-PARC. By substituting the pulse width transmitted by the supermirror-coated slit package into $\Delta t_{\rm ch}$ in Eq. (4), we can estimate the energy resolution of 4SEASONS equipped with the supermirror-coated slit package. As shown in Fig. 11, the energy resolution becomes almost constant ($\sim 5\%$) in the wide range of incident energy, which is also consistent with our prediction.

The energy dependence of the intensity gain of the supermirror-coated slit package is shown in Fig. 12. The integrated intensities of a supermirror-coated slit package are divided by that

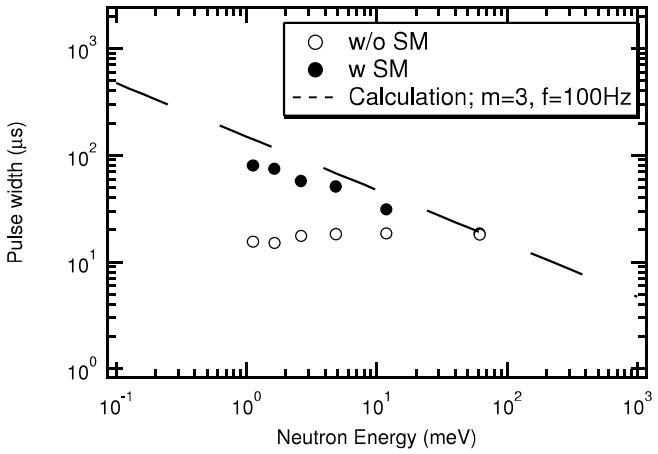

Figure 10. Energy dependence of pulse widths in the case of rotating slit packages with and without neutron supermirrors ($m = 3$). The rotation frequency is 100 Hz for both the cases. The calculated result from Eq. (1) is also plotted.

of the slit package without neutron supermirrors. The gain factor at around 1 meV reaches approximately 20. Until now, the Fermi chopper has never been intended for monochromating such slow neutrons due to the finite depth of slit package. This study demonstrated that a supermirror-coated slit package can monochromate the slow neutrons with high transmission, which confirm that an instrument with the MAGIC chopper can provide superior performance over the wide energy range from cold to epithermal neutron energies.

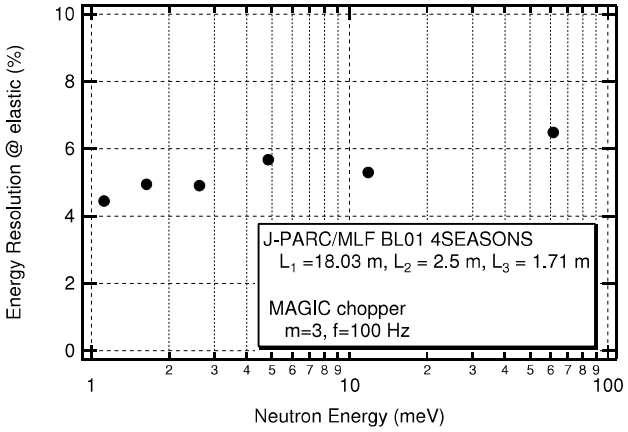

Figure 11. Estimated energy resolution at the elastic position for the Fermi chopper spectrometer 4SEASONS containing the supermirror-coated slit package described in this paper.

5. Conclusion

We proposed to apply a supermirror-coated slit package to monochromating chopper (MAGIC chopper) in order to optimize the experimental conditions for each of incident energies in INS experiment on pulsed neutron source. It is found that a rotating supermirror-coated slit package increases the effective chopper opening time in a lower energy region, which confirms that the MAGIC chopper can overcome the difficulty in the optimization problem of INS experiment with Multi-E_i method. Furthermore, the intensity gain obtained by a supermirror-coated slit package is found to reach 20 at $E \sim 1$ meV. This study experimentally proved that the MAGIC chopper can significantly improve the measurement efficiency of INS experiment by a chopper spectrometer, and thus contribute to open up a new field of materials science.

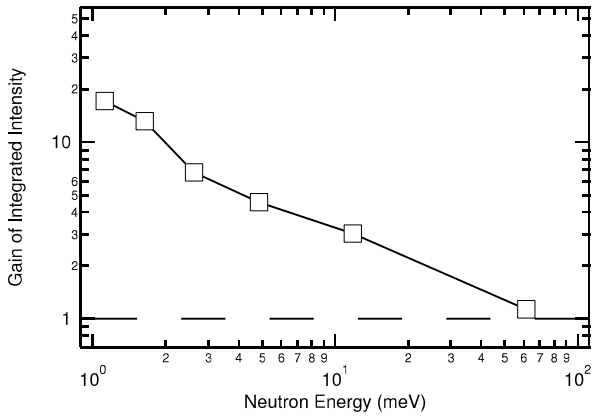

Figure 12. Integrated intensity gain for the supermirror-coated slit package ($m = 3$). The rotation frequency is 100 Hz. All values in the figure are normalized by the integrated intensities for a rotating slit package without neutron supermirrors.

Acknowledgement

This work was supported by a Grant-in-Aid for Specially Promoted Research (No. 17001001) from the Ministry of Education, Culture, Sports, Science and Technology, Japan, and a Grant in-Aid for Scientific Research (C) (No. 20612016) from the Japan Society for the Promotion of Science. The experiment on NOBORU was conducted under Project No. 2009A0083.

References

[1] Mezei F 1997 *J. Neutron Research* **6** 3
[2] Mezei F, Russina M, Schorr S 2000 Physica B **276-278** 128
[3] Nakamura M, Nakajima K, Kajimoto R, Arai M 2007 *J. Neutron Research* **15** 31
[4] Russina M and Mezei F 2009 *Nucl. Instrum. Methods Phys. Res.* A **604** 629
[5] Nakamura M, Kajimoto R, Inamura Y, Mizuno F, Fujita M, Yokoo T, Arai M 2009 *J. Phys. Soc. Jpn.* **78** 093002
[6] Iida K, Kofu M, Katayama N, Lee J, Kajimoto R, Inamura Y, Nakamura M, Arai M, Yoshida Y, Fujita M, Yamada K, Lee S H 2011 *Phys. Rev.* B **84** 060402(R)
[7] Kajimoto R, Nakajima K, Ohira-Kawamura S, Kakurai K, Arai M, Hokazono T, Oozono S, Okuda T 2010 *J. Phys. Soc. Jpn.* **79** 123705
[8] Ishikado M, Nagai Y, Kodama K, Kajimoto R, Nakamura M, Inamura Y, Wakimoto S, Nakamura H, Machida M, Suzuki K, Usui H, Kuroki K, Iyo A, Eisaki E, Arai M and Shamoto S 2011 *Phys. Rev.* B **84** 144517
[9] Nakamura M, Arai M, Kajimoto R, Yokoo T, Nakajima K and Krist Th 2008 *J. Neutron Research* **16** 87
[10] Nakamura M, Kambara W, Krist Th, Shinohara T, Ikeuchi K, Arai M, Kajimoto R, Nakajima K, Tanaka H, Suzuki J, Harada M, Oikawa K and Maekawa F 2014 *Nucl. Instrum. Methods Phys. Res.* A **737** 142
[11] http://j-parc.jp/researcher/MatLife/en/instrumentation/ns3.html
[12] Oikawa K, Maekawa F, Harada M, Kai T, Meigo S, Kasugai Y, Ooi M, Sakai K, Teshigawara M, Hasegawa S, Futakawa M, Ikeda Y, Watanabe N 2008 *Nucl. Instrum. Methods Phys. Res.* A **589** 310
[13] Maekawa F, Oikawa K, Harada M, Kai T, Meigo S, Kasugai Y, Ooi M, Sakai K, Teshigawara M, Hasegawa S, Ikeda Y, Watanabe N 2009 *Nucl. Instrum. Methods Phys. Res.* A **600** 335
[14] Kajimoto R, Nakamura M, Inamura Y, Mizuno F, Nakajima K, Ohira-Kawamura S, Yokoo T, Nakatani T, Maruyama R, Soyama K, Shibata K, Suzuya K, Sato S, Aizawa K, Arai M, Wakimoto S, Ishikado M, Shamoto S, Fujita M, Hiraka H, Ohoyama K, Yamada K, Lee D H 2011 *J. Phys. Soc. Jpn.* **80** SB025